



UNIVERSITY OF LEEDS

This is a repository copy of *Modelling heavy metals contamination in groundwater of Southern Punjab, Pakistan*.

White Rose Research Online URL for this paper:

<https://eprints.whiterose.ac.uk/166770/>

Version: Accepted Version

Article:

Ashraf, A, Chen, X orcid.org/0000-0002-2053-2448 and Ramamurthy, R (2021) Modelling heavy metals contamination in groundwater of Southern Punjab, Pakistan. *International Journal of Environmental Science and Technology*, 18 (8). pp. 2221-2236. ISSN 1735-2630

<https://doi.org/10.1007/s13762-020-02965-w>

© Islamic Azad University (IAU) 2020. This is an author produced version of an article published in *International Journal of Environmental Science and Technology*. Uploaded in accordance with the publisher's self-archiving policy.

Reuse

Items deposited in White Rose Research Online are protected by copyright, with all rights reserved unless indicated otherwise. They may be downloaded and/or printed for private study, or other acts as permitted by national copyright laws. The publisher or other rights holders may allow further reproduction and re-use of the full text version. This is indicated by the licence information on the White Rose Research Online record for the item.

Takedown

If you consider content in White Rose Research Online to be in breach of UK law, please notify us by emailing eprints@whiterose.ac.uk including the URL of the record and the reason for the withdrawal request.



eprints@whiterose.ac.uk
<https://eprints.whiterose.ac.uk/>

Modelling Heavy Metals Contamination in Groundwater of Southern Punjab, Pakistan

A. Ashraf^{1,2*}, **X. Chen**², **R. Ramamurthy**¹

¹UNESCO-IHE Institute for Water Education, Westvest 7, 2611 AX, Delft, Netherlands

²School of Civil Engineering, University of Leeds, LS2 9JT, Leeds, United Kingdom

*Corresponding author:

Full Name, Adil Ashraf

Address, Professor Evertslaan 88 A, 2628 XX, Delft, Netherlands

Email, ashraf_adil@outlook.com

Tel, +44 (0) 7741919998

Acknowledgements

The corresponding author acknowledges the Commonwealth Scholarship Commission and the University of Leeds for proffering the opportunity to pursue this research work as a Commonwealth Shared Scholar to fulfil partially the requirement for the degree of MSc (Eng) in Environmental Engineering and Project Management.

Declarations

Funding

This study was funded by the Commonwealth Scholarship Commission and the University of Leeds.

Conflicts of Interest

The authors declare that they have no conflict of interest.

Availability of Data and Material

Not applicable.

Code Availability

Not applicable.

Abstract

The present study aimed to develop a numerical simulation to predict the chemistry change of groundwater heavy metals pollution (mainly arsenic pollution) in the Southern region of the Punjab province of Pakistan. This work is the first attempt in modelling the transport of groundwater heavy metals pollution in the area using a 1D reactive transport model. PHREEQC was employed to perform the numerical simulation. The conceptual model represented the 1D numerical transport model with the homogenous mineral composition having uniform transport of the municipal wastewater. A 100 m column - 20 cell transport model was used with a time step of 5,000 years; making a simulated timescale of 100,000 years. The simulation was carried out using quartz, illite, and calcite kinetics. Arsenic sorption kinetics were also incorporated in the simulation. The results revealed that the concentrations of four out of ten heavy metals and three out of eight inorganic ions were above the drinking water quality standards at the end of the simulation making the groundwater unsafe for drinking purposes. The arsenic concentration was found out to be 3.79 mg/l against 100,000 year which is 379 times the international drinking water standard and about 76 times the national drinking water standard for arsenic. It is concluded that the groundwater, regardless of the natural soil treatment, will be highly contaminated after 100,000 years particularly with heavy metals including arsenic, cadmium, iron, lead, and nickel. The groundwater quality can be enhanced by appreciating the preventive measures recommended in this study.

Keywords

Arsenic · Geochemistry · Contamination · Groundwater · Modelling

Introduction

Heavy metals groundwater contamination is an emerging issue in Pakistan. The concentration of heavy metals increases in soil due to the discharge of untreated wastewater from agricultural, industrial, and municipal sources. This subsequently leads to heavy metals accumulation in groundwater. Heavy metals concentrations in groundwater throughout the country often exceed the World Health Organisation (WHO) permissible drinking water limits (Raza et al. 2017; Waseem et al. 2014). The exceeding amount of toxic metals can severely degrade groundwater quality resulting in adverse human health problems (Azizullah et al. 2011). Groundwater arsenic contamination is becoming a serious human health problem in Asian countries (Ravenscroft et al. 2009) exclusively in Pakistan (Podgorski et al. 2017) and China (Deng et al. 2009). Higher arsenic concentration is carcinogenic to humans and causes skin, lung, liver, and/or kidney cancers (Mahar et al. 2013). The groundwater arsenic concentration exceeded the WHO guideline value of 10 µg/l in several regions of the country particularly in the Punjab and Sindh provinces (Azizullah et al. 2011; Raza et al. 2017; Waseem et al. 2014). The Pakistan Council of Research in Water Resources (PCRWR) conducted numerous studies across the country. The studies revealed that a large number of drinking water samples exceed the WHO guideline value for arsenic concentration in the Punjab and Sindh provinces (Raza et al. 2017). More than 50 million people in Pakistan were recently reported to be at the risk of arsenic groundwater pollution (Podgorski et al. 2017). Generally, the heavy metals exceed the permissible limits in Pakistan except for lead, zinc, and copper (Raza et al. 2017).

Rigorous geochemical modelling together with the understanding of heavy metals geochemistry and hydrogeology are of utmost significance for conceiving an appropriate, sustainable and cost-effective solution for groundwater preservation (Ghosh and Singh 2009). The computer models have largely been employed for evaluating the chemistry change and anticipating the behaviour change of groundwater under various geochemical and hydrogeological conditions (Chidambaram et al. 2012). PHREEQC is a computer software that can be used for executing a range of geochemical simulations including one dimensional (1D) transport modelling. The programme can simulate chemical transport processes in natural and polluted water and also for industrial processes and laboratory experiments. It is based on the chemistry of aqueous solutions at equilibrium state interrelating with minerals, ion exchangers, and sorption surfaces; with the ability to model 1D transport and kinetic processes (Charlton and Parkhurst 2011; Parkhurst and Appelo 2013).

The present study has therefore been conducted to predict the chemistry change of groundwater heavy metals pollution with the focus on arsenic pollution using PHREEQC in the Southern region of the Punjab province of Pakistan for a timescale of 100,000 years. This work is the first attempt in modelling the transport of groundwater

heavy metals pollution in the study area with the help of a 1D reactive transport model. The long-time prediction (e.g. 100,000 years) will provide a clear understanding of the heavy metal pollution evolution process, especially for some slow kinetics reaction process. With a better understanding of the transport process of heavy metals, this research will help the industry/government policymakers in developing methods to restore the contaminated soil and groundwater.

Materials and Methods

Study Area

Mailsi is a tehsil in the Punjab province of Pakistan. It is situated in the district Vehari, in Southern Punjab between 72°17' - 72°19' East and 29°78' - 29°92' North (**Fig. 1**). The tehsil has a population of about 0.95 million as per 2017 census (PBS 2017). It covers an area of 1,639 km² with an elevation of around 126 m above sea level. It has mostly arid to semi-arid climate with an average temperature of about 26°C and an average annual precipitation of about 242 mm. Majority of the population is dependent on farming for livelihood. The major cash crops are wheat, sugarcane, cotton, rice, and maize. The area is located alongside River Sutlej. However, the river is mostly reported dry and therefore this area lacks sufficient amount of safe drinking water. Groundwater is the major source of drinking water in the area. It is mostly being exploited using hand or electric pumps (Rasool et al. 2016a; Rasool et al. 2016b).

The aquifer in this area is under alluvial plains having more than 340 m thick layer of Pleistocene and Holocene sediments. These sediments are transported by the River Sutlej (Greenman et al. 1967) arising from Kailash mountains adjacent to the Mansarovarand Lake which moves parallel to the Himalayas. High concentrations of clay, silt, and fine sand and low organic content are associated with these sediments. There is a thickened layer of unconsolidated flood plain deposits in the area alongside old deposits of Pleistocene to present age (Farooq et al. 2007). The south-western part of the study area comprises of comparatively older alluvial deposits which incline to coincide with highly mineralised groundwater regions (Greenman et al. 1967). The factors affecting the transmissibility and permeability of water are disparity in sand thickness, lateral lithological variations, and grain size distribution (Farooq et al. 2007). The wide distribution of older Pleistocene deposits stimulates aerobic conditions in the aquifer in the western part of the study area (Tasneem 1999).

Mineral Composition

The backfill mineral composition (**Table 1**) is taken from Shahid et al. (2013). The composition against the city of Multan is used as it is considered to be a representative composition for the study area. The primary minerals

are quartz (68.8%), illite (14.14%) and chamosite (10.26%). Other reported mineral phases are calcite, vermiculite, dolomite, epidote, albite, chlorochlore, gypsum, talcum, and aluminate.

Aquifer Characteristics

The properties of a homogeneous sandy aquifer are presented in **Table 2**. The dispersivity affects the chemical transport and therefore needs to be as realistic as possible. The longitudinal dispersivity is used in the numerical transport modelling. The value of 5.06 m is taken for longitudinal dispersivity. This value is calculated elsewhere (Shakoor et al. 2017). Gelhar et al. (1992) reported a range of 3.0 - 15.24 m for longitudinal dispersivity after reviewing several researches, whereas Engesgaard et al. (1996) reported a range of 1.0 - 10 m for longitudinal dispersivity.

Contaminated Influent Solution

The influent solution is presumed to be municipal wastewater having typical values from characterisation studies (**Table 3**). All the values are derived from (Rehman et al. 2008; Sial et al. 2006) except the concentration of cadmium, cobalt, chromium, nitrate, and sulphate which are assumed to be having the same values as the background solution.

Background Filling Solution

The background solution (**Table 4**) is adopted from the groundwater characterisation studies conducted in tehsil Mailsi (Rasool et al. 2016a; Rasool et al. 2016b). Results from both the studies were analysed and the arithmetic means values were taken for all the parameters to have a representative solution for the study area.

Modelling Approach

PHREEQC was employed to perform the numerical simulation. The simulation is carried out using kinetics for quartz, illite, and calcite minerals. Other minerals are excluded due to their limited influence on the geochemical and hydrogeological processes. Arsenic sorption kinetics are also incorporated in the numerical simulation.

Reactive Transport

Flow from Darcy's Law is used in the transport modelling. The general transport equation (Appelo and Postma 2004) can be expressed as:

$$\frac{\partial(\phi C_i)}{\partial t} = \frac{\partial [\phi D_{\alpha\beta}^i \frac{\partial C_i}{\partial x_\beta}]}{\partial x_\alpha} - \frac{\partial(u_\alpha C_i)}{\partial x_\alpha} + Q$$

Where, C_i = the i th component

u_α = the Darcy velocity in the α direction

ϕ = the aquifer porosity

Q = the sorption or reaction term

Mineral Kinetics

Quartz Dissolution

Quartz is a primary mineral found in the study area. It is a silicate mineral which dissolves either partially or wholly depending on solution characteristics. The dissolution of quartz in water produces H_4SiO_4 in its simplest form. The dissolution rate is dependent on pH and temperature (Chen et al. 2015; Crundwell 2014).

The general rate equation (Appelo and Postma 2004) can be expressed as:

$$R_k = r_k \frac{A_o}{V} \left(\frac{m_k}{m_{ok}} \right)^n$$

Where, r_k = the specific rate of reaction

A_o = the initial surface area (m^2)

V = the solution volume (kgw)

m_k/m_{ok} = the solid moles at a given time to the initial solid moles

n = 0.67 for uniformly dissolving spheres and cubes

The specific rate reaction for quartz (Worley 1994) can be expressed as:

$$r_k = K(1 - SR)$$

Where, K = the constant

= $10e-13.7 \text{ mol.m}^{-2}.\text{s}^{-1}$ at 25°C (Palandri and Kharaka 2004)

SR = the saturation ratio

The quartz dissolution is initially dependent on the groundwater silicon concentration. The higher silicon concentration in the groundwater is the result of quartz dissolution.

Illite Dissolution

Illite dissolves either partially or completely depending on solution characteristics. The dissolution rate is dependent on pH. Köhler et al. (2003) comprehensively investigated the dissolution kinetics of illite.

The general rate equation is:

$$R_k = [2.2 \times 10^{-4} \times e^{\frac{-46}{RT}} \times a(H^+)^{0.6}] + [2.5 \times 10^{-13} \times e^{\frac{-14}{RT}}] + [0.27 \times e^{\frac{-67}{RT}} \times a(OH^-)^{0.6}]$$

Where, R = the gas constant [$8314 \text{ KJ.mol}^{-1}.\text{K}^{-1}$]

T = the temperature in Kelvin [298 K]

Calcite Dissolution/Precipitation

Calcite dissolution or precipitation is based on rate equations taken from Plummer et al. (1978).

The forward rate equation can be expressed as:

$$r_f = K_1[H^+] + K_2[CO_2(aq)] + K_3[H_2O]$$

Where, K_1, K_2, K_3 = the temperature-dependent rate coefficients

The backward rate equation can be expressed as:

$$r_b = K_4[Ca^{2+}][HCO_3^{2-}] = K_4[Ca^{2+}]^2$$

Where, K_4 = the rate coefficient dependent on the composition of the solution

The overall rate for calcite [$r_f - r_b$] in a pure calcite-water system can be expressed as:

$$r_{Calcite} = r_f \left[1 - \left(\frac{IAP}{K_{Calcite}} \right)^{2/3} \right]$$

Where, r_f = the forward rate

$IAP/K_{Calcite}$ = the saturation ratio

The overall kinetic reaction rate provided by Appelo and Postma (2004) is used with the specific rate for calcite provided above.

Arsenic Sorption

The sorption mechanism can be explained by using one of the isotherms such as Langmuir, Freundlich, Polanyi, and Brunauer. The system characteristics govern the appropriate model for a specific component. Freundlich and Langmuir isotherms are mostly used for single-solute sorption (Jeong 2005).

Data related to sorption can be described reasonably well by the Freundlich model. The empirical formula of it (Limousin et al. 2007) can be expressed as:

$$S = K.C^n$$

Where, S = the mass of adsorbate per mass of adsorbent [mg/g]

K = the partition coefficient [l/g]

C = the pollutant concentration [mg/l]

n = the degree of nonlinearity [1.0 or <1.0]

Sorption parameters can be taken from the literature, laboratory column experiments, or field studies. Several researchers reviewed and compiled the sorption parameters for arsenic for various sorbent materials (Kanel et al. 2006; Moghal et al. 2017). The partition coefficient value of 0.50 l/kg is adopted for the numerical simulation (Moghal et al. 2017).

The adopted sorption equation (Tebes-Stevens et al. 1998) is:

$$R = -K_m (C - (S/K))$$

Where, R = the sorption rate [mol/l.h]

- K_m = the mass transfer coefficient [1/h (h-hours)]
- C = the pollutant concentration [mol/l]
- S = the sorbed pollutant concentration [mol/g]
- K = the partition coefficient [l/g]

Conceptual Model

The conceptual model represents a 1D numerical transport model with the homogenous mineral composition having uniform transport of the municipal wastewater. A 100 m column - 20 cell transport model has been used with a time step of 5,000 years; making a simulated timescale of 100,000 years (**Fig. 2**). The wastewater is injected from the left side with outflow from the right side. The required modelling parameters are provided in **Table 5**. The PHREEQC programme file used in numerical modelling is provided in the supplementary material.

Results and Discussion

Evolution of pH Behaviour

The pH starts from the neutral value of 7.0 and it marginally increases with time until it reaches the value of 7.5 at 100,000 year (**Fig. 3a**). The rationale behind this increment is the addition of quartz which releases the hydroxide (OH^-) ions. On the contrary, against the column distance, the pH shows an overall decreasing trend to realise an equilibrium for the timeline of 100,000 years (**Fig. 3b, 3c, 3d**). It can be associated with minerals weathering, geochemical activities, and sorption/desorption processes. Also, the pH reaches an equilibrium within the 100 m column length in the first 50,000 years whereas the pH does not realise a plateau within the 100 m column length in the next 50,000 years. This is due to the increasing value of pH at the initial distance of 2.5 m with the increase of the simulation time.

Power of hydrogen (pH) is the degree of the balance of acids and alkalis in the environment. There are various factors that can affect the pH values including acids, alkalis, carbon dioxide, chlorine, sodium hypochlorite, and calcium hypochlorite (Tribe 2017). The pH controls the arsenic sorption/desorption processes which in turn influence the arsenic mobilisation and transformation processes. Most toxic cation metals adsorption (to hydrous metal oxides) increases with the increase of pH value due to becoming highly insoluble at higher pH value. Nevertheless, the adsorption of oxyanions like arsenate tends to be limited with the increase of pH value (Smedley and Kinniburgh 2002).

The relationship of pH values with the respective arsenic concentrations during the timescale of 5 – 100 thousand years is shown in **Fig. 4a**. The R-squared value for the linear trend line was found out to be 0.99. The arsenic concentrations slightly reduce with the increase in the pH values. This can be related with the increase in the

arsenic sorption as the pH increases (**Fig. 4b**). Raven et al. (1998) investigated the arsenite and arsenate adsorption by changing pH values, illustrating that the adsorption of arsenate was higher at lower pH and the adsorption of arsenite was higher at pH value of more than 7.5. Mapoma et al. (2016) studied the arsenic mobilisation using reactive transport groundwater hydrochemistry modelling, mentioning that the lower pH range favours the arsenic immobilisation and therefore reducing arsenic in the system.

Evolution of Heavy Metals Behaviour

Arsenic is a toxic component characterised as a metalloid. It is ubiquitous and present in soil, water, and atmosphere. It is commonly found in the environment as arsenic-containing minerals such as arsenopyrite (FeAsS), realgar (AsS), arsenolite (As₂O₃), and orpiment (As₂S₃). It can either be mobilised naturally or anthropogenically in the natural waters. Nevertheless, the risk of contaminations due to anthropogenic activities has increased manifold in the recent decades. The anthropogenic effect can either be direct due to point source discharges or indirect by enabling geochemical processes resulting in release of arsenic. The geochemical parameters that control the arsenic speciation and mobilisation in the subsurface environments are pH, redox potential, competing ions, organic matter, soil phase mineralogy, and microbial activities. These factors influence the arsenic concentration by stirring processes such as oxidation, reduction, dissolution, precipitation, bioaccumulation, adsorption, and desorption. The processes that could lead to groundwater arsenic contamination due to transformation and mobilisation from solid to solution phase are oxidative weathering, reductive dissolution, and alkaline desorption. Reduction and dissolution cause arsenic release in reducing conditions whilst desorption mobilises arsenic due to high pH and/or competing ions in oxidising conditions. Adsorption with iron oxides also plays a key role in controlling the arsenic concentrations (Hafeznezami 2015).

The arsenic concentration begins from the value of 1.34e-6 mol/l (100 µg/l) and it increases sharply at the first step and then it shows a plateau for the first 25,000 years. After that, it decreases with time until it reaches the value of 5.06e-5 mol/l (3,795 µg/l) at 100,000 year. This decrement is due to the sorption of arsenic. There is generally an increasing trend of the arsenic sorption with time. The arsenic sorption increases with time to 75,000 year and then it slightly decreases to 100,000 year as illustrated in **Fig. 4c**.

The relationship of arsenic with the respective arsenic sorption concentrations during the time period of 5 – 100 thousand years is shown in **Fig. 4d**. The arsenic concentrations slightly decrease with the increase in the sorption. The relationship of arsenic with the respective pH values during the time period of 5 – 100 thousand years is shown in **Fig. 5a**. The arsenic concentration remains constant at the pH value of about 7.0 for the first 25,000 years and then it slightly decreases with the increase in the pH value.

The arsenic shows an overall increasing trend with the column distance to realise an equilibrium for the timeline of 100,000 years (**Fig. 5b, 5c, 5d**). It can be associated with minerals weathering, geochemical activities, and sorption/desorption processes (Liu et al. 2013; Welch et al. 2000). Mapoma et al. (2016) studied the trend for arsenic against the column distance (of 250 m) for simulation time (of 1,000 year), showing the comparatively fluctuation patterns owing to the dissimilar model design and parameterisation.

Arsenic speciation and mobilisation is controlled by the pH, the redox potential, the presence of competing ions, and the mineral characteristics. Arsenic mobilisation and sorption distribution have been investigated in several studies under various aspects (Hafeznezami 2015; Lawson et al. 2013; Mai et al. 2014; Mapoma et al. 2016; Neidhardt et al. 2014; Omoregie et al. 2013; Polya et al. 2005; Postma et al. 2007; Quicksall et al. 2008; Radloff et al. 2011; Ravenscroft et al. 2009; Rowland et al. 2007). Arsenic can adsorb on iron oxides, aluminium oxides, manganese oxides, calcite, mackinawite, and clay minerals (Herath et al. 2016; Roman-Ross et al. 2006). The adsorbed arsenic concentration decreases in the presence of competing anions such as bicarbonate and phosphate (Appelo et al. 2002). The adsorption mechanism is usually pH dependent. The elevated arsenic concentrations can be associated with the arsenic release in the system due to mobilisation at higher pH value (of above 8.5) (Dixit and Hering 2003; Smedley and Kinniburgh 2002).

Arsenic removal from the system depends on various factors such as pH of the medium, arsenic oxidation state, and redox potential. The chemical removal technologies include oxidation, coagulation or chemical precipitation, adsorption, ion exchange, and membrane processes. These removal processes can either be used simultaneously or sequentially in the conventional removal technologies (Mohanty 2017). The selection of the technology depends on arsenic mobilisation and transformation; presence of chemical constituents like phosphate, silica, iron, and sulphate; hardness; and cost (Litter et al. 2010). The most important factor in selecting the removal process is the composition and chemistry of arsenic in the system (Singh et al. 2015). The available methods are more effective for arsenate (Johnston and Heijnen 2015). Therefore, a two-step removal approach with arsenite oxidation to arsenate followed by an arsenate removal technology is considered to be efficient for arsenic removal (Pous et al. 2015).

Cadmium usually occurs in the divalent form (Cd(II)) in aqueous solutions (Alloway 2012). It mainly mobilises in oxic and acidic environments. Cadmium sorption is aggravated by high concentrations of hydrous oxides, organic matter, and clay minerals (Lin et al. 2016). The geochemical parameters that can further affect its mobility are pH, redox potential, and solution ionic strength. Cadmium is one of the heavy metals that are mobile in the environment as it can remain as water-soluble complexes in solution and does not precipitate like the many other

heavy metals (Loganathan et al. 2012). The higher mobilisation potential through ligand and competition persuaded desorption is the rationale behind the faster cadmium release into groundwater from soil. Kubier et al. (2019) provided a broad overview of the hydro-chemical behaviour of cadmium in soil and groundwater with various studies investigating the release of cadmium. The cadmium concentration starts from the value of 6.2391×10^{-7} mol/l ($69.878 \mu\text{g/l}$) and it is constant for first 25,000 years and then it decreases with time until it reaches the value of 6.2345×10^{-7} mol/l ($69.826 \mu\text{g/l}$) at 100,000 year. However, against the column distance, the cadmium indicates an overall increasing trend to realise an equilibrium for the timeline of 100,000 years due to minerals weathering, and geochemical processes.

Iron exists either as Fe(II) or Fe(III) in the forms of iron oxides, oxy-hydroxides, and hydroxides. It is moderately abundant in natural environments such as rocks, groundwater, and soils. Iron oxides are considered as good adsorbents for ions (Cornell and Schwertmann 2003). They are usually used as an adsorbent to treat water or gas. Arsenate can strongly be adsorbed on iron oxides and ultimately be removed from contaminated water (Mohan and Pittman Jr 2007). It is a relatively inexpensive remediation option. Some iron oxides express high sorption affinity for both arsenite and arsenate (Aredes et al. 2013; Khan and Ho 2011). The materials that are able to remove both arsenite and arsenate from water are goethite, amorphous iron oxyhydroxides, and ferrihydrite (Lafferty and Loeppert 2005). The iron concentration begins from 2.01×10^{-5} mol/l ($1,126 \mu\text{g/l}$) and it is constant for first 20,000 years and then it increases with time until it reaches the value of 3.48×10^{-5} mol/l ($1,949 \mu\text{g/l}$) at 100,000 year. With the column distance, iron expresses a decreasing trend to realise an equilibrium for the timeline of 100,000 years. This decrement can be due to the arsenic sorption on iron oxides and the consequent precipitation of those oxides such as hematite ($\alpha\text{-Fe}_2\text{O}_3$), maghemite ($\beta\text{-Fe}_2\text{O}_3$), and magnetite (Fe_3O_4). It can also be associated with minerals weathering, and geochemical processes. Mapoma et al. (2016) studied the trend for iron against the column distance (of 250 m) for a simulation time of 1,000 year, showing the comparatively fluctuating patterns owing to the dissimilar model design and parameterisation.

Manganese occurs in two main forms Mn(II) and Mn(IV) in the aqueous environments. The conversion between the two forms occurs through oxidation and reduction reactions. The chemistry of manganese largely depends on pH and redox states. It can be leached from minerals and soils (WHO 2004). Manganese oxides have strong sorption capacities. The oxides of manganese can have an impact on the geochemistry of arsenic (Schacht and Ginder-Vogel 2018). The manganese starts at 1.82×10^{-7} mol/l ($10 \mu\text{g/l}$) and it is constant for first 10,000 years and then it increases with time until it reaches the value of 2.87×10^{-6} mol/l ($158 \mu\text{g/l}$) at 100,000 year. However, against the column distance, the manganese illustrates an overall decreasing trend to realise an equilibrium for the timeline

of 100,000 years. It can be associated with minerals weathering, and geochemical processes. Mapoma et al. (2016) studied the trend for manganese against the column distance (of 250 m) for simulation time (of 1,000 year), showing the comparatively fluctuation patterns owing to the dissimilar model design and parameterisation.

The predicted behaviours throughout the timescale for heavy metals are provided in **Fig. 6a and 6b**. The prominent patterns in particular are of arsenic, iron, zinc, and copper. These patterns can be associated with mineral phases geochemistry. The comparison of heavy metals concentrations at the end of the simulation time with the drinking water quality standards is provided in **Table 6**. The values of four out of ten heavy metals are well above the standards making the water unsafe for drinking water supplies. The value of arsenic is found out to be 3.79 mg/l at 97.5 m for 100,000 year. The value is 379 times the WHO standard for arsenic and about 76 times the PEQS standard for arsenic. The groundwater is shown to be highly contaminated with arsenic, cadmium, iron, lead, and nickel.

Evolution of Water Controlling Metal Ions Behaviour

Bicarbonate contributes to the alkalinity of the medium. It helps in regulating the pH and the metal content. Bicarbonate and carbonate ions can remove toxic metals such as cadmium, and lead through precipitation. It can also influence the arsenic mobilisation. Higher concentration of bicarbonate in groundwater can release/mobilise arsenic from aquifer sediments. It is considered as an important mechanism of groundwater arsenic mobilisation (Anawar et al. 2004). It varies significantly with the existence of cations and redox environments (Henke 2009). The concentration of bicarbonate at the start is 9.90×10^{-3} mol/l (604 mg/l) and then it is constant at 9.93×10^{-3} mol/l (606 mg/l) for next three steps (5,000 - 15,000 years). After that, the concentration decreases with time until it reaches the value of 4.32×10^{-3} mol/l (264 mg/l) at 100,000 year. The reason can be the increase of saturation index of some of the carbonate/bicarbonate minerals with time. The mineral precipitates at positive saturation index which subsequently decreases the respective component concentration. On the contrary, against the column distance, the concentration demonstrates an overall increasing trend to achieve an equilibrium for the timeline of 100,000 years.

Calcium is an alkaline-earth metal and is the fifth most abundant element in the Earth's crust. It is mostly found as a divalent cation with +2 oxidation state and is generally produces inorganic salts such as calcium carbonate, calcium phosphate, and others. It can react with oxygen forming oxides and with water forming hydroxides. It plays an important role in geological processes (Perrone and Monteiro 2016). The availability of inorganics such as calcium affects the arsenic sorption in soils (Wang and Mulligan 2006). The concentration of calcium at the start is 2.47×10^{-3} mol/l (99 mg/l) and then it is constant at 2.50×10^{-3} mol/l (100 mg/l) for first 20,000 years. After that,

the concentration decreases with time until it reaches the value of $1.44\text{e-}3$ mol/l (58 mg/l) at 100,000 year. On the contrary, against the column distance, the calcium concentration shows an overall increasing pattern to realise an equilibrium for the timeline of 100,000 years mainly due to the calcite dissolution.

Nitrate is an important polyatomic ion. It can influence arsenic mobilisation and transformation. The principal source of arsenic in the environment is the oxidation of arsenic-containing sulphide minerals, such as pyrite (FeS_2). It is thought to be as an important source of groundwater arsenic contamination (Welch et al. 2000). It takes place through several reactions including in the presence of nitrate at $\text{pH} > 5.0$ (Ahmed et al. 2004). The nitrate concentration at the start is $2.00\text{e-}3$ mol/l (124 mg/l) and then it is constant at $1.90\text{e-}3$ mol/l (118 mg/l) for next seven steps (5,000 - 40,000 years). After that, the concentration slightly increases with time until it reaches the value of $1.96\text{e-}3$ mol/l (122 mg/l) at 100,000 year. On the contrary, against the column distance, the concentration shows an overall decreasing trend to achieve an equilibrium for the timeline of 100,000 years.

Sulphate can mobilise arsenic in groundwater by influencing the arsenic sorption/desorption processes. The elevated concentrations of sulphate in overlying water initiates the arsenic desorption from aquifer sediments. Sulphate competes with arsenate and arsenite for adsorption sites on iron oxides. This reduces the adsorbed arsenic amount on mineral surfaces and stimulates the arsenic dissolution in sediments. Sulphate can also be utilised by microorganisms to promote the release of arsenic. The sulphate-reducing microorganisms initiate iron oxides reduction resulting in arsenic desorption. The sulphate concentrations are therefore important for controlling the arsenic contamination in the groundwater (Li et al. 2018). The concentration of sulphate at the start is $5.3918\text{e-}3$ mol/l (518 mg/l) and it is constant until 20,000 years. After that, the concentration slightly decreases with time until it reaches the value of $5.3878\text{e-}3$ mol/l (517 mg/l) at 100,000 year. With the column distance, the concentration shows an increasing trend to achieve an equilibrium for the timeline of 100,000 years.

The predicted behaviours throughout the timescale for water controlling ions are provided in **Fig. 7a and 7b**. The prominent patterns in particular are of bicarbonate, sodium, and chloride. These patterns can be associated with mineral phases dissolution and precipitation. The comparison of water containing ions concentrations at the end of the simulation time with the drinking water quality standards is provided in **Table 7**. The values of three out of eight inorganic ions are well above the standards making the water unsafe for drinking water supplies. The three ions are nitrate, sulphate, and potassium.

Conclusion

The groundwater of Tehsil Mailsi is characterised by high levels of arsenic, cadmium, iron, lead, nickel, nitrate, sulphate, and potassium with slightly alkaline pH and lower levels of manganese after 100,000 year. The

groundwater is shown to be highly contaminated particularly with heavy metals posing a serious risk to both public health and environmental quality. Arsenic speciation and mobilisation is controlled by the pH, the redox potential, the presence of competing ions, and the mineral characteristics. These factors influence the arsenic concentration by stirring processes such as oxidation, reduction, dissolution, precipitation, bioaccumulation, adsorption, and desorption. Arsenic can adsorb on oxides of iron, aluminium, and manganese, and also on calcite, mackinawite, and clay minerals. The adsorbed arsenic concentration decreases in the presence of competing anions such as bicarbonate and phosphate. Technologies such as oxidation, coagulation or chemical precipitation, adsorption, ion exchange, and membrane filtration can be explored for the effective arsenic removal.

The areas of research that can be explored in future are: heavy metals leaching studies based on laboratory column tests along with geochemical and hydrogeological evaluations to validate the modelling outcomes by correlating the experimental results with the modelling results; assessment of remediation methods through groundwater heavy metals contamination modelling; and influence of enhanced adsorption and precipitation on arsenic removal using reactive transport modelling.

Conflict of Interest

The authors declare that they have no conflict of interest.

References

- Ahmed KM, Bhattacharya P, Hasan MA, Akhter SH, Alam SM, Bhuyian MH, Imam MB, Khan AA, Sracek O (2004) Arsenic enrichment in groundwater of the alluvial aquifers in Bangladesh: An overview. *J. Appl. Geochem* 19:181-200. <https://doi.org/10.1016/j.apgeochem.2003.09.006>
- Akhter G, Hasan M (2016) Determination of aquifer parameters using geoelectrical sounding and pumping test data in Khanewal district, Pakistan. *Open Geosci* 8:630-638. <https://doi.org/10.1515/geo-2016-0071>
- Alloway BJ (2012) *Heavy metals in soils: Trace metals and metalloids in soils and their bioavailability*. Springer Science and Business Media
- Anawar HM, Akai J, Sakugawa H (2004) Mobilization of arsenic from subsurface sediments by effect of bicarbonate ions in groundwater. *Chemosphere* 54:753-762. <https://doi.org/10.1016/j.chemosphere.2003.08.030>
- Appelo C, Weiden MVD, Tournassat C, Charlet L (2002) Surface complexation of ferrous iron and carbonate on ferrihydrite and the mobilization of arsenic. *Environ. Sci. Technol.* 36:3096-3103. <https://doi.org/10.1021/es010130n>
- Appelo CAJ, Postma D (2004) *Geochemistry, groundwater and pollution*. CRC Press
- Aredes S, Klein B, Pawlik M (2013) The removal of arsenic from water using natural iron oxide minerals. *J. Clean. Prod.* 60:71-76. <https://doi.org/10.1016/j.jclepro.2012.10.035>
- Azizullah A, Khattak MNK, Richter P, Häder D-P (2011) Water pollution in Pakistan and its impact on public health - A review. *Environ. Int.* 37:479-497. <https://doi.org/10.1016/j.envint.2010.10.007>
- Charlton SR, Parkhurst DL (2011) Modules based on the geochemical model PHREEQC for use in scripting and programming languages. *Comput Geosci* 37:1653-1663. <https://doi.org/10.1016/j.cageo.2011.02.005>
- Chen X, Thornton SF, Small J (2015) Influence of hyper-alkaline pH leachate on mineral and porosity evolution in the chemically disturbed zone developed in the near-field host rock for a nuclear waste repository. *Transport Porous Med* 107:489-505. <https://doi.org/10.1007/s11242-014-0450-0>
- Chidambaram S, Anandhan P, Prasanna MV, Ramanathan AL, Srinivasamoorthy K, Senthil Kumar G (2012) Hydrogeochemical modelling for groundwater in Neyveli aquifer, Tamil Nadu, India, Using PHREEQC: A case study. *Nat. Resour. Res.* 21:311-324. <https://doi.org/10.1007/s11053-012-9180-6>
- Cornell RM, Schwertmann U (2003) *The iron oxides: Structure, properties, reactions, occurrences and uses*. John Wiley and Sons

- Crundwell FK (2014) The mechanism of dissolution of minerals in acidic and alkaline solutions (Part II): Application of a new theory to silicates, aluminosilicates and quartz. *Hydrometallurgy* 149:265-275. <http://dx.doi.org/10.1016/j.hydromet.2014.07.003>
- Deng Y, Wang Y, Ma T (2009) Isotope and minor element geochemistry of high arsenic groundwater from Hangjinhouqi, the Hetao Plain, Inner Mongolia. *J. Appl. Geochem.* 24:587-599. <https://doi.org/10.1016/j.apgeochem.2008.12.018>
- Dixit S, Hering JG (2003) Comparison of arsenic (V) and arsenic (III) sorption onto iron oxide minerals: Implications for arsenic mobility. *Environ. Sci. Technol.* 37:4182-4189. <https://doi.org/10.1021/es030309t>
- Engesgaard P, Jensen KH, Molson J, Frind EO, Olsen H (1996) Large-scale dispersion in a sandy aquifer: Simulation of subsurface transport of environmental tritium. *Water Resour. Res.* 32:3253-3266. <https://doi.org/10.1029/96WR02398>
- Farooq A, Yousafzai MA, Jan MQ (2007) Hydro-geochemistry of the Indus Basin in Rahim Yar Khan District, Central Pakistan. *J Chem Soc Pakistan* 29:525-537
- Gelhar LW, Welty C, Rehfeldt KR (1992) A critical review of data on field-scale dispersion in aquifers. *Water Resour. Res.* 28:1955-1974. <https://doi.org/10.1029/92WR00607>
- Ghosh N, Singh R (2009) Groundwater arsenic contamination in india: vulnerability and scope for remedy. Citeseer
- Greenman DV, Swarzenski WV, Benet DG (1967) Groundwater hydrology of Punjab, West Pakistan with emphasis on problems caused by canal irrigation. USAID
- Hafeznezami S (2015) Arsenic mobilization and sorption in subsurface environments: Experimental studies, geochemical modeling, and remediation strategies. Dissertation, University of California
- Henke KR (2009) Environmental chemistry, health threats and waste treatment. John Wiley and Sons
- Herath I, Vithanage M, Bundschuh J, Maity JP, Bhattacharya P (2016) Natural arsenic in global groundwaters: Distribution and geochemical triggers for mobilization. *Curr. Pollut. Rep.* 2:68-89. <https://doi.org/10.1007/s40726-016-0028-2>
- Jeong Y (2005) The adsorption of arsenic (V) by iron (Fe₂O₃) and aluminum (Al₂O₃) oxides. Dissertation, Iowa State University
- Johnston R, Heijnen H (2015) Safe water technology for arsenic removal.

- Kanel SR, Choi H, Kim JY, Vigneswaran S, Shim WG (2006) Removal of arsenic (III) from groundwater using low-cost industrial by-products-blast furnace slag. *Water Qual Res J* 41:130-139. <https://doi.org/10.2166/wqrj.2006.015>
- Khan MA, Ho Y-s (2011) Arsenic in drinking water: A review on toxicological effects, mechanism of accumulation and remediation. *Asian J. Chem.* 23:1889
- Köhler SJ, Dufaud F, Oelkers EH (2003) An experimental study of illite dissolution kinetics as a function of pH from 1.4 to 12.4 and temperature from 5 to 50 C. *Geochim. Cosmochim. Acta* 67:3583-3594. [https://doi.org/10.1016/S0016-7037\(03\)00163-7](https://doi.org/10.1016/S0016-7037(03)00163-7)
- Kubier A, Wilkin RT, Pichler T (2019) Cadmium in soils and groundwater: A review. *J. Appl. Geochem.* 104388. <https://doi.org/10.1016/j.apgeochem.2019.104388>
- Lafferty BJ, Loeppert R (2005) Methyl arsenic adsorption and desorption behavior on iron oxides. *Environ. Sci. Technol.* 39:2120-2127. <https://doi.org/10.1021/es048701+>
- Lawson M, Polya DA, Boyce AJ, Bryant C, Mondal D, Shantz A, Ballentine CJ (2013) Pond-derived organic carbon driving changes in arsenic hazard found in asian groundwaters. *Environ. Sci. Technol.* 47:7085-7094. <https://doi.org/10.1021/es400114q>
- Li S, Yang C, Peng C, Li H, Liu B, Chen C, Chen B, Bai J, Lin C (2018) Effects of elevated sulfate concentration on the mobility of arsenic in the sediment – Water interface. *Ecotox Environ Safe* 154:311-320. <https://doi.org/10.1016/j.ecoenv.2018.02.046>
- Limousin G, Gaudet JP, Charlet L, Szenknect S, Barthès V, Krimissa M (2007) Sorption isotherms: A review on physical bases, modeling and measurement. *J. Appl. Geochem.* 22:249-275. <https://doi.org/10.1016/j.apgeochem.2006.09.010>
- Lin Z, Schneider A, Sterckeman T, Nguyen C (2016) Ranking of mechanisms governing the phytoavailability of cadmium in agricultural soils using a mechanistic model. *Plant Soil* 399:89-107. <https://doi.org/10.1007/s11104-015-2663-6>
- Litter MI, Morgada ME, Bundschuh J (2010) Possible treatments for arsenic removal in latin american waters for human consumption. *Environ. Pollut.* 158:1105-1118. <https://doi.org/10.1016/j.envpol.2010.01.028>
- Liu CC, Kar S, Jean JS, Wang CH, Lee YC, Sracek O, Li Z, Bundschuh J, Yang HJ, Chen CY (2013) Linking geochemical processes in mud volcanoes with arsenic mobilization driven by organic matter. *J. Hazard. Mater.* 262:980-988. <https://doi.org/10.1016/j.jhazmat.2012.06.050>

- Loganathan P, Vigneswaran S, Kandasamy J, Naidu R (2012) Cadmium sorption and desorption in soils: A review. *Crit Rev Env Sci Tec* 42:489-533. <https://doi.org/10.1080/10643389.2010.520234>
- Mahar MT, Khuhawar MY, Jahangir TM, Baloch MA (2013) Health risk assessment of heavy metals in groundwater: The effect of evaporation ponds of distillery spent wash. *J Environ Eng Sci* 2:166
- Mai NTH, Postma D, Trang PTK, Jessen S, Viet PH, Larsen F (2014) Adsorption and desorption of arsenic to aquifer sediment on the red river floodplain at Nam Du, Vietnam. *Geochimica et Cosmochimica Acta* 142:587-600. <https://doi.org/10.1016/j.gca.2014.07.014>
- Mapoma HWT, Xie X, Pi K, Liu Y, Zhu Y (2016) Understanding arsenic mobilization using reactive transport modeling of groundwater hydrochemistry in the Datong Basin Study Plot, China. *Environ Sci Process Impacts* 18:371-385
- Moghal AAB, Reddy KR, Mohammed SAS, Al-Shamrani MA, Zahid WM (2017) Retention studies on arsenic from aqueous solutions by lime treated semi-arid soils. *Int J Geomate* 12:17-24
- Mohan D, Pittman Jr CU (2007) Arsenic removal from water/wastewater using adsorbents - A critical review. *J. Hazard. Mater.* 142:1-53. <https://doi.org/10.1016/j.jhazmat.2007.01.006>
- Mohanty D (2017) Conventional as well as emerging arsenic removal technologies — A critical review. *Water Air Soil Poll.* 228:381. <https://doi.org/10.1007/s11270-017-3549-4>
- Neidhardt H, Berner ZA, Freikowski D, Biswas A, Majumder S, Winter J, Gallert C, Chatterjee D, Norra S (2014) Organic carbon induced mobilization of iron and manganese in a west bengal aquifer and the muted response of groundwater arsenic concentrations. *Chem. Geol.* 367:51-62. <https://doi.org/10.1016/j.chemgeo.2013.12.021>
- Omeregic EO, Couture RM, Cappellen PV, Corkhill CL, Charnock JM, Polya DA, Vaughan D, Vanbroekhoven K, Lloyd JR (2013) Arsenic bioremediation by biogenic iron oxides and sulfides. *Appl. Environ. Microbiol.* 79:4325-4335. <https://aem.asm.org/content/79/14/4325>
- Palandri JL, Kharaka YK (2004) A compilation of rate parameters of water-mineral interaction kinetics for application to geochemical modeling. USGS
- Parkhurst DL, Appelo C (2013) Description of input and examples for PHREEQC (Version 3): A computer program for speciation, batch-reaction, one-dimensional transport, and inverse geochemical calculations. USGS. <https://doi.org/10.3133/tm6A43>
- PBS (2017) Province wise provisional results of census - 2017. Pakistan Bureau of Statistics, Government of Pakistan. <http://www.pbs.gov.pk/>

- Perrone D, Monteiro M (2016) Chapter 5: The chemistry of calcium. The Royal Society of Chemistry
- Plummer LN, Wigley TML, Parkhurst DL (1978) The Kinetics of calcite dissolution in CO₂ - Water systems at 5 degrees to 60 degrees C and 0.0 to 1.0 atm CO₂. *Am. J. Sci.* 278:179-216
- Podgorski JE, Eqani SAMAS, Khanam T, Ullah R, Shen H, Berg M (2017) Extensive arsenic contamination in high-pH unconfined aquifers in the Indus Valley. *Sci. Adv.* 3
- Polya DA, Gault AG, Diebe N, Feldman P, Rosenboom JW, Gilligan E, Fredericks D, Milton AH, Sampson M, Rowland HAL, Lythgoe PR (2005) Arsenic hazard in shallow cambodian groundwaters. *Mineral. Mag.* 69:807-823
- Postma D, Larsen F, Hue NTM, Duc MT, Viet PH, Nhan PQ, Jessen S (2007) Arsenic in groundwater of the Red River floodplain, Vietnam: Controlling geochemical processes and reactive transport modeling. *Geochimica et Cosmochimica Acta* 71:5054-5071. <https://doi.org/10.1016/j.gca.2007.08.020>
- Pous N, Casentini B, Rossetti S, Fazi S, Puig S, Aulenta F (2015) Anaerobic arsenite oxidation with an electrode serving as the sole electron acceptor: A novel approach to the bioremediation of arsenic-polluted groundwater. *J. Hazard. Mater.* 283:617-622. <https://doi.org/10.1016/j.jhazmat.2014.10.014>
- Quicksall AN, Bostick BC, Sampson M (2008) Linking organic matter deposition and iron mineral transformations to groundwater arsenic levels in the Mekong Delta, Cambodia. *J. Appl. Geochem.* 23:3088-3098. <https://doi.org/10.1016/j.apgeochem.2008.06.027>
- Radloff KA, Zheng Y, Michael HA, Stute M, Bostick BC, Mihajlov I, Bounds M, Huq MR, Choudhury I, Rahman MW, Schlosser P (2011) Arsenic migration to deep groundwater in Bangladesh influenced by adsorption and water demand. *Nat. Geosci.* 4:793. <https://doi.org/10.1038/ngeo1283>
- Rasool A, Farooqi A, Xiao T, Masood S, Kamran MA, Bibi S (2016a) Elevated levels of arsenic and trace metals in drinking water of Tehsil Mailsi, Punjab, Pakistan. *J. Geochem. Explor.* 169:89-99. <https://doi.org/10.1016/j.gexplo.2016.07.013>
- Rasool A, Xiao T, Farooqi A, Shafeeqe M, Masood S, Ali S, Fahad S, Nasim W (2016b) Arsenic and heavy metal contaminations in the tube well water of Punjab, Pakistan and risk assessment: A case study. *Ecol. Eng.* 95:90-100. <https://doi.org/10.1016/j.ecoleng.2016.06.034>
- Raven KP, Jain A, Loeppert RH (1998) Arsenite and arsenate adsorption on ferrihydrite: Kinetics, equilibrium, and adsorption envelopes. *Environ. Sci. Technol.* 32:344-349. <https://doi.org/10.1021/es970421p>
- Ravenscroft P, Brammer H, Richards K (2009) Arsenic pollution: A global synthesis. John Wiley and Sons

- Raza M, Hussain F, Lee J-Y, Shakoor MB, Kwon KD (2017) Groundwater status in Pakistan: A review of contamination, health risks, and potential needs. *Crit Rev Environ Sci Technol* 47:1713-1762. <https://doi.org/10.1080/10643389.2017.1400852>
- Rehman W, Zeb A, Noor N, Nawaz M (2008) Heavy metal pollution assessment in various industries of Pakistan. *Environ. Geol.* 55:353-358. <https://doi.org/10.1007/s00254-007-0980-7>
- Roman-Ross G, Cuello G, Turrillas X, Fernandez-Martinez A, Charlet L (2006) Arsenite sorption and co-precipitation with calcite. *Chem. Geol.* 233:328-336. <https://doi.org/10.1016/j.chemgeo.2006.04.007>
- Rowland HAL, Pederick RL, Polya DA, Pancost RD, Dongen BEV, Gault AG, Vaughan DJ, Bryant C, Anderson B, Lloyd J.R (2007) The control of organic matter on microbially mediated iron reduction and arsenic release in shallow alluvial aquifers, Cambodia. *Geobiology* 5:281-292. <https://doi.org/10.1111/j.1472-4669.2007.00100.x>
- Schacht L, Ginder-Vogel M (2018) Arsenite depletion by manganese oxides: A case study on the limitations of observed first order rate constants. *Soil Systems* 2:39. <https://doi.org/10.3390/soilsystems2030039>
- Shahid M, Awan M, Hussain K (2013) Mineralogy of major soils of Punjab (Pakistan) by X-Ray diffraction. *Int. J. Agric. Sci.* 2:265-272
- Shakoor A, Khan ZM, Arshad M, Farid HU, Sultan M, Azmat M, Shahid MA, Hussain Z (2017) Regional groundwater quality management through hydrogeological modeling in LCC, West Faisalabad, Pakistan. *J. Chem.*
- Shieh HY, Chen JS, Lin CN, Wang WK, Liu CW (2010) Development of an artificial neural network model for determination of longitudinal and transverse dispersivities in a convergent flow tracer test. *J. Hydrol* 391:367-376. <https://doi.org/10.1016/j.jhydrol.2010.07.041>
- Sial R, Chaudhary M, Abbas S, Latif M, Khan A (2006) Quality of effluents from Hattar industrial estate. *J. Zhejiang Univ. Sci. B* 7:974-980. <https://doi.org/10.1631/jzus.2006.B0974>
- Singh R, Singh S, Parihar P, Singh VP, Prasad SM (2015) Arsenic contamination, consequences and remediation techniques: A review. *Ecotox Environ Safe* 112:247-270. <https://doi.org/10.1016/j.ecoenv.2014.10.009>
- Smedley PL, Kinniburgh D (2002) A review of the source, behaviour and distribution of arsenic in natural waters. *J. Appl. Geochem.* 17:517-568. [https://doi.org/10.1016/S0883-2927\(02\)00018-5](https://doi.org/10.1016/S0883-2927(02)00018-5)
- Sracek O (2013) Applications of geochemical modeling and reactive transport modeling in the evaluation of environmental impact of mining: PHREEQC program input files. Palacký University

- Tasneem MA (1999) Impact of agricultural and industrial activities on groundwater quality in Kasur area. *J Pak Atom E Com* 36:175-180
- Tebes-Stevens C, Valocchi JA, Briesen JMV, Rittmann BE (1998) Multicomponent transport with coupled geochemical and microbiological reactions: Model description and example simulations. *J. Hydrol* 209:8-26. [https://doi.org/10.1016/S0022-1694\(98\)00104-8](https://doi.org/10.1016/S0022-1694(98)00104-8)
- Tribe C (2017) What Variables Affect pH Levels? *Sciencing*
- Wang S, Mulligan CN (2006) Effect of natural organic matter on arsenic release from soils and sediments into groundwater. *Environ. Geochem. Health* 28:197-214. <https://doi.org/10.1007/s10653-005-9032-y>
- Waseem A, Arshad J, Iqbal F, Sajjad A, Mehmood Z, Murtaza G (2014) Pollution status of Pakistan: A retrospective review on heavy metal contamination of water, soil, and vegetables. *Biomed Res. Int.*
- Welch AH, Westjohn DB, Helsel DR, Wanty RB (2000) Arsenic in Ground Water of the United States: Occurrence and Geochemistry *Groundwater* 38:589-604
- WHO (2004) Manganese and its compounds: Environmental aspects. World Health Organisation
- Worley WG (1994) Dissolution kinetics and mechanisms in quartz and granite-water systems. Dissertation, Massachusetts Institute of Technology

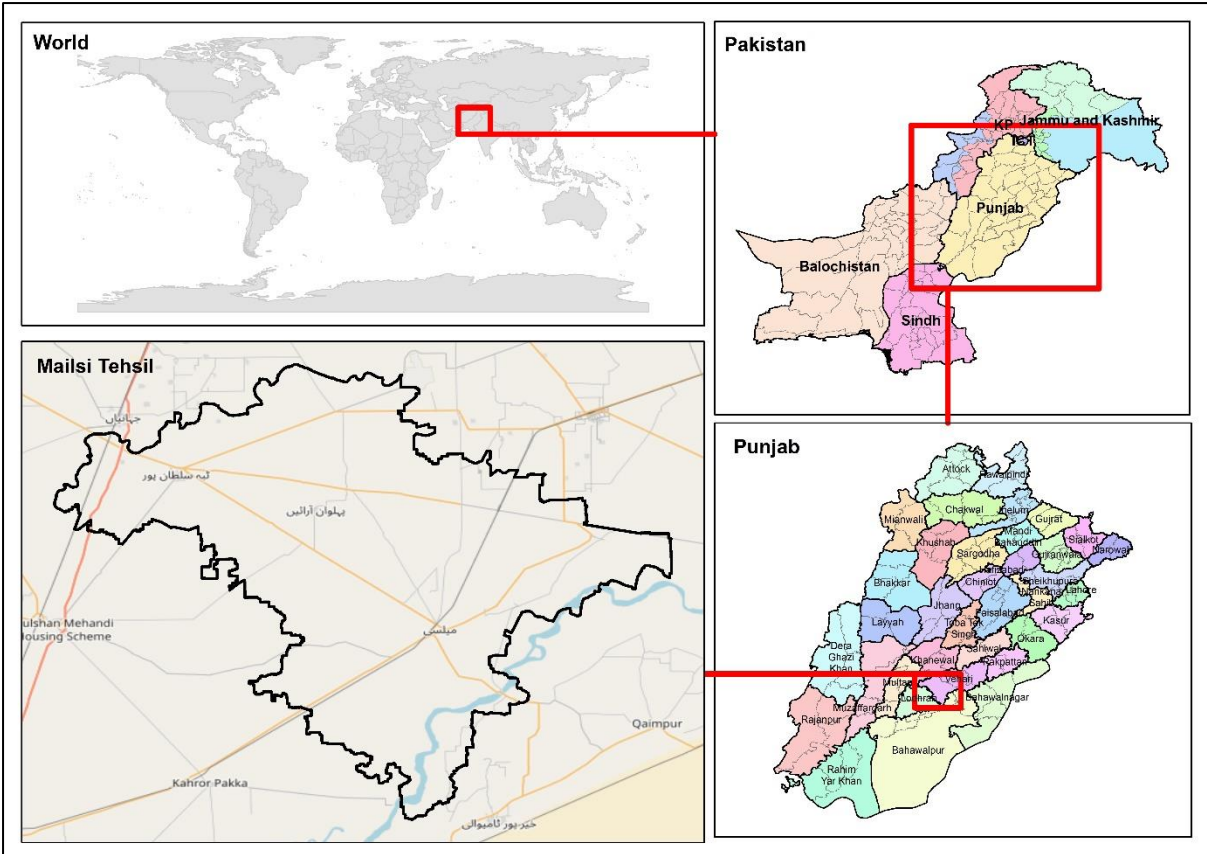


Fig. 1 Key location map of the study area

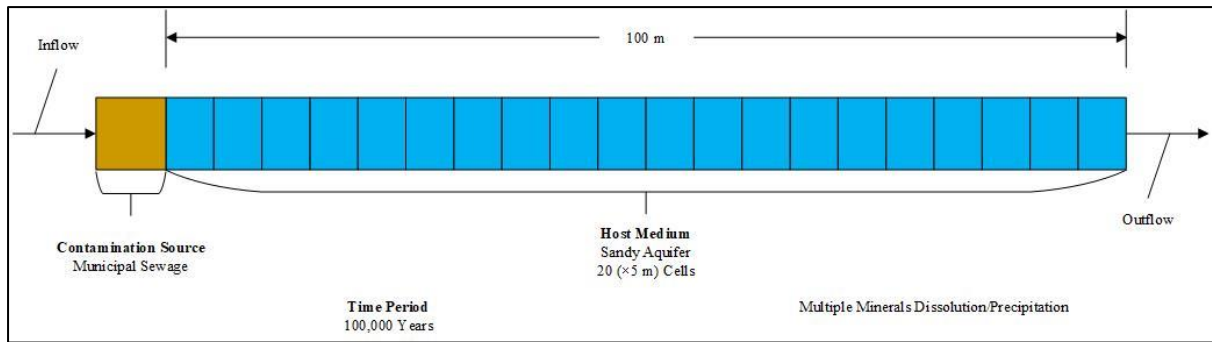


Fig. 2 Conceptual model for numerical transport modelling

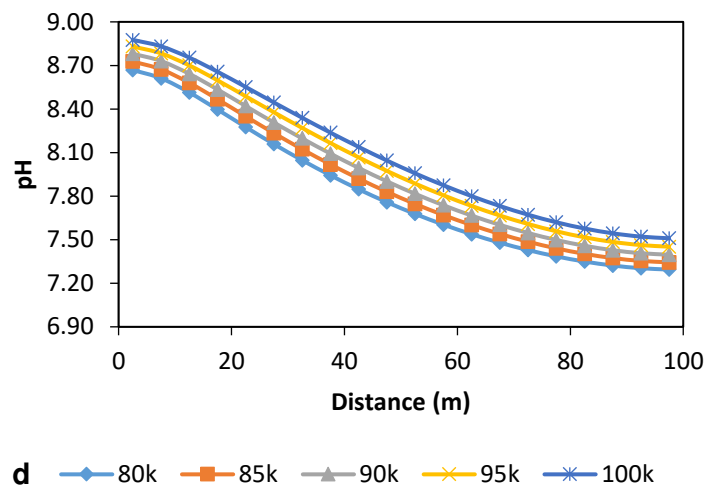
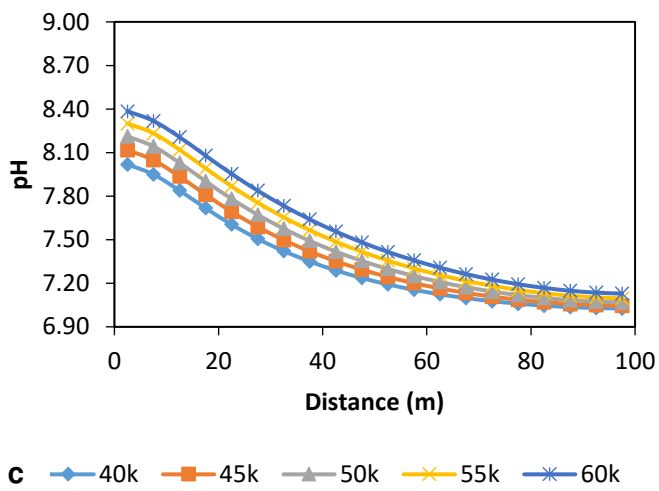
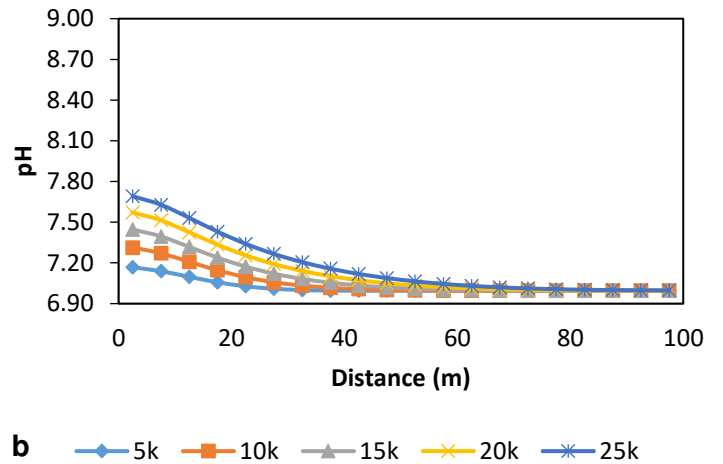
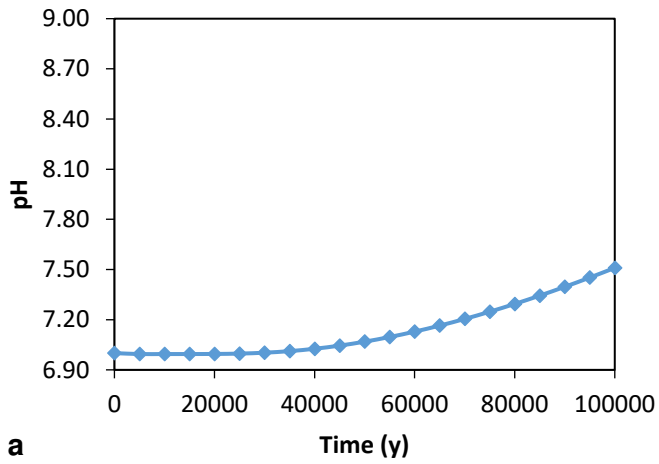
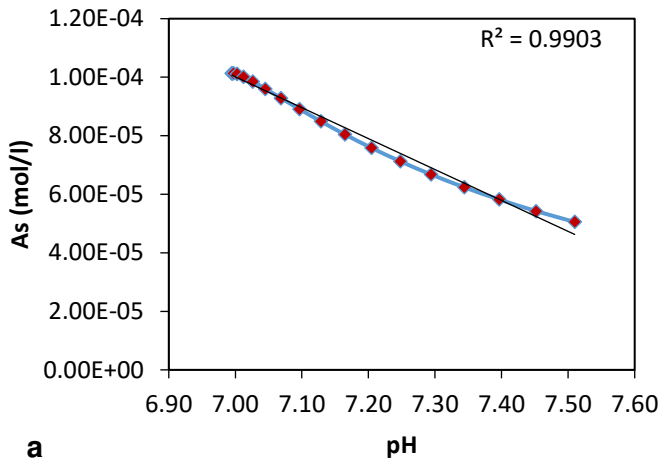
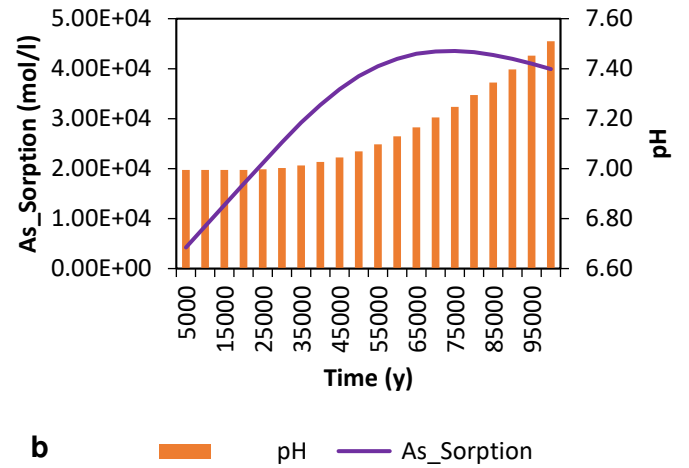


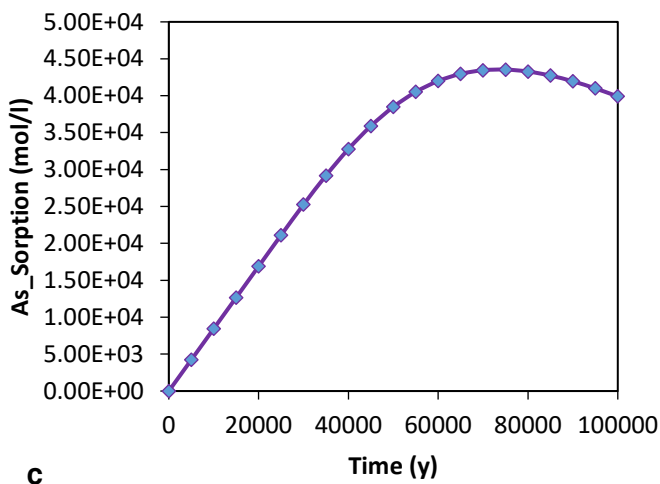
Fig. 3 **a** Predicted pH behaviour throughout the simulation timescale, **b** Predicted temporal variation of pH behaviour for 5,000 – 25,000 years, **c** Predicted temporal variation of pH behaviour for 40,000 – 60,000 years, **d** Predicted temporal variation of pH behaviour for 80,000 – 100,000 years



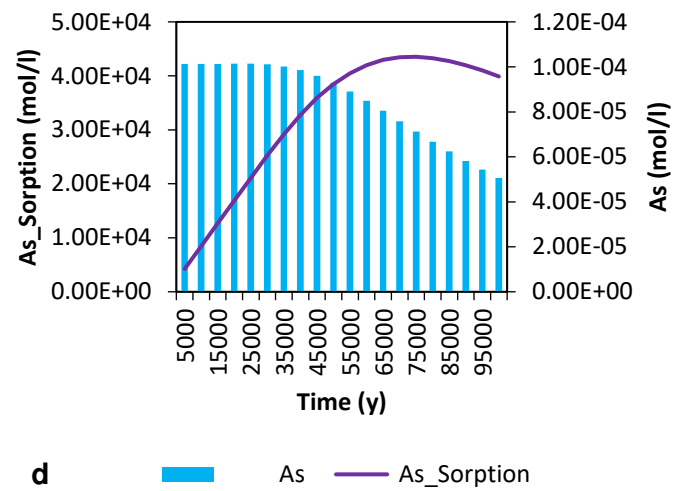
a



b

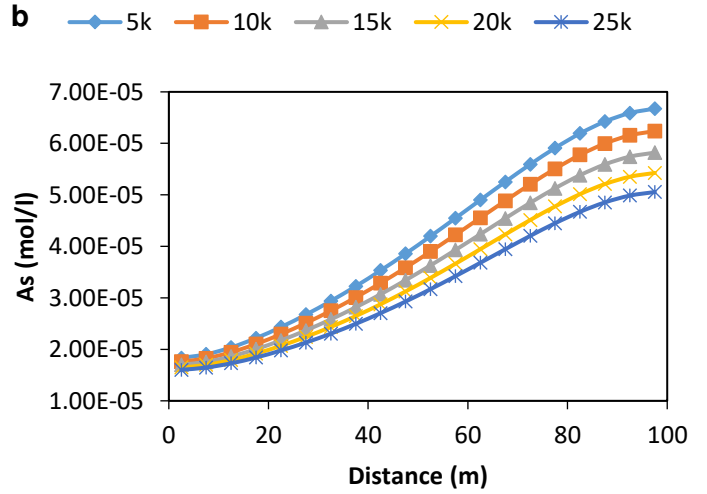
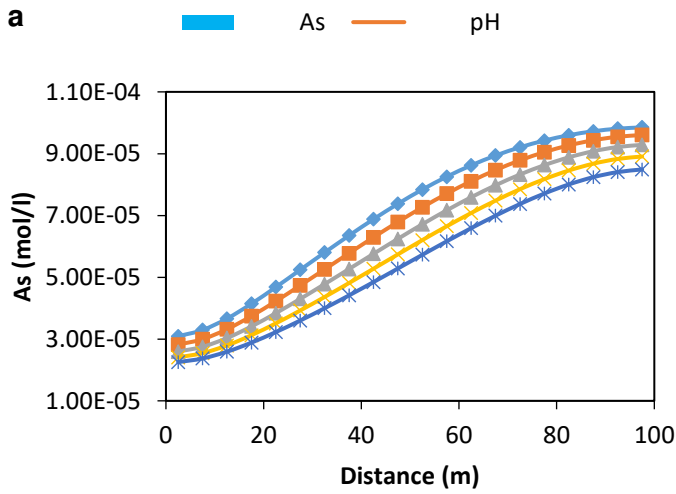
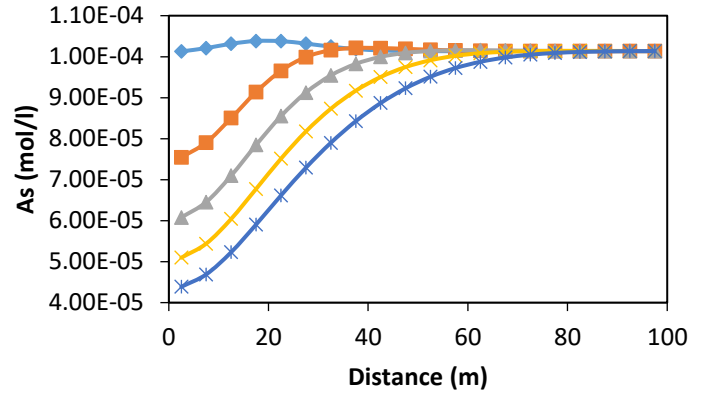
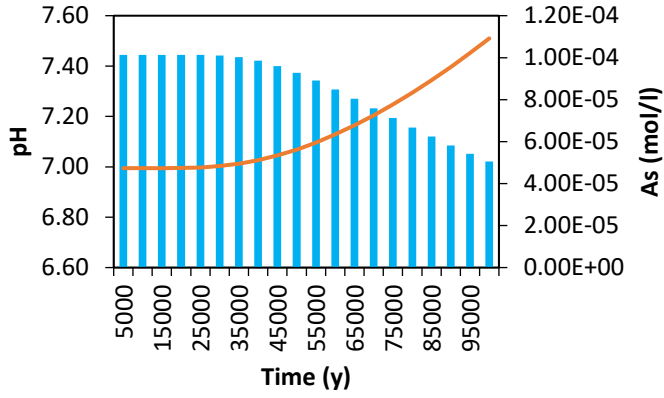


c



d

Fig. 4 a Relationship between pH and arsenic concentration during the simulation timescale of 5,000 – 100,000 years, **b** Relationship between pH and arsenic sorption during the simulation timescale of 5,000 – 100,000 years, **c** Arsenic sorption concentration at the column outlet during the simulation timescale of 5,000 – 100,000 years, **d** Relationship between arsenic and arsenic sorption during the simulation timescale of 5,000 – 100,000 years



c —◆— 40k —■— 45k —▲— 50k —×— 55k —*— 60k

d —◆— 80k —■— 85k —▲— 90k —×— 95k —*— 100k

Fig. 5 a Relationship between arsenic and pH during the simulation timescale of 5,000 – 100,000 years, **b** Predicted temporal variation of arsenic behaviour for 5,000 – 25,000 years, **c** Predicted temporal variation of arsenic behaviour for 40,000 – 60,000 years, **d** Predicted temporal variation of arsenic behaviour for 80,000 – 100,000 years

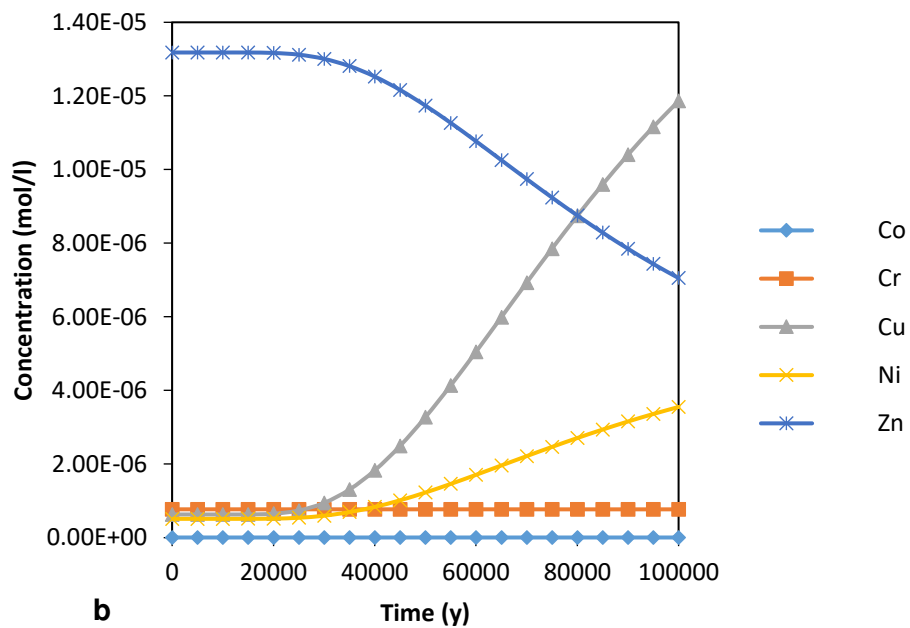
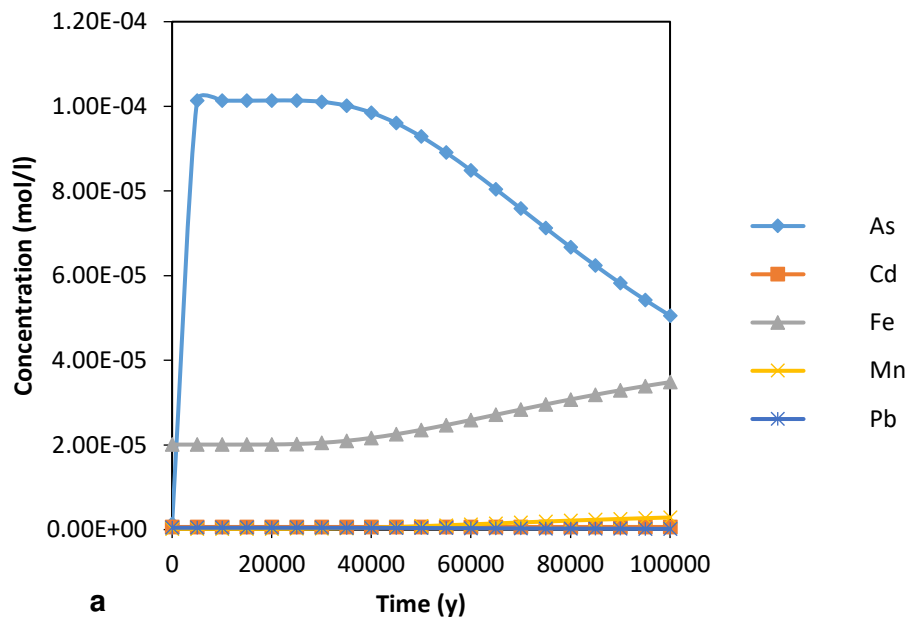


Fig. 6 a Predicted temporal variation of arsenic, cadmium, iron, manganese and lead behaviours throughout the simulation timescale of 100,000 years, **b** Predicted temporal variation of cobalt, chromium, copper, nickel and zinc behaviours throughout the simulation timescale of 100,000 years

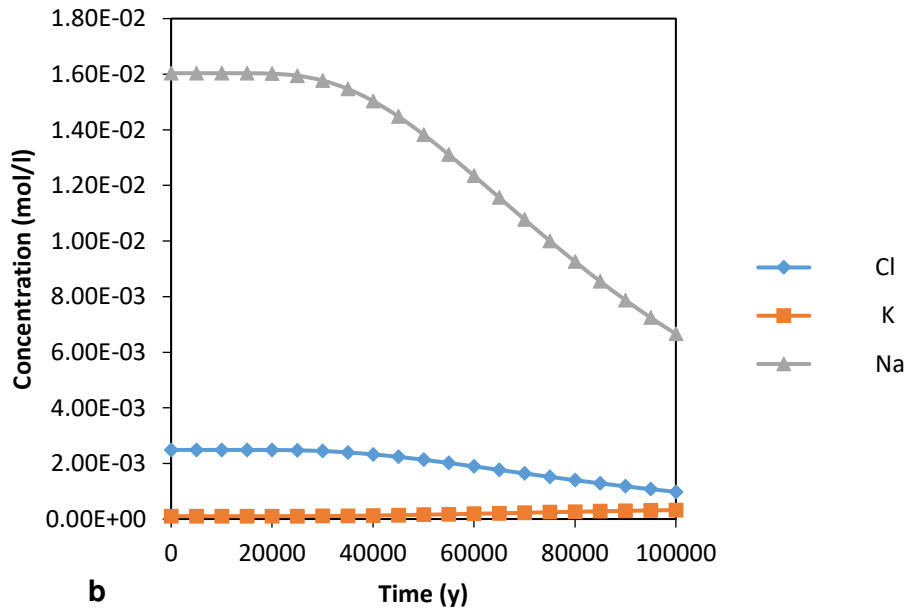
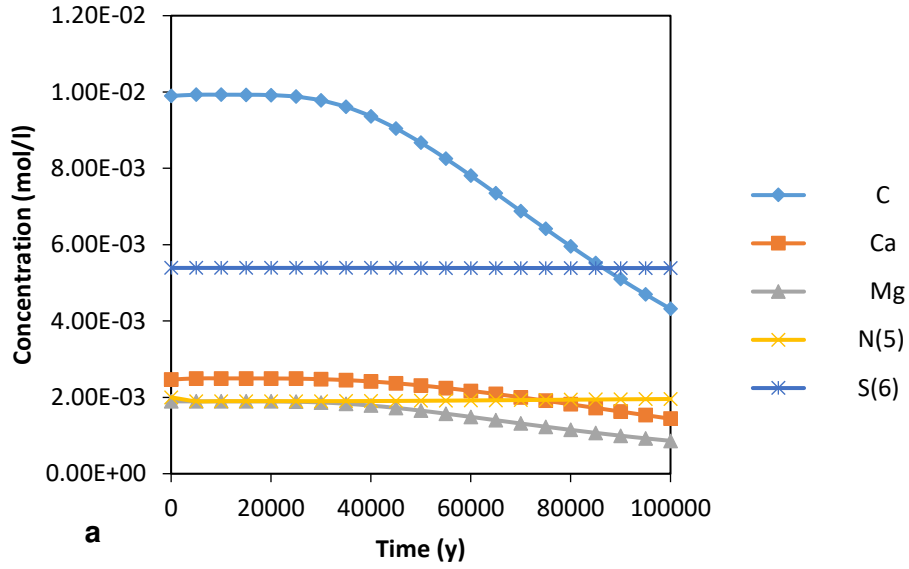


Fig. 7 a Predicted temporal variation of bicarbonate, calcium, magnesium, nitrate and sulphate behaviours throughout the simulation timescale of 100,000 years, **b** Predicted temporal variation of chloride, potassium and sodium behaviours throughout the simulation timescale of 100,000 years

Table 1 Backfill mineral composition and conceptualisation for numerical simulation (Shahid et al. 2013)

Mineral	Formula	Composition (%)	Modelling
Quartz	SiO ₂	68.83	Modelled
Illite	(KH ₃ O)Al ₂ Si ₃ AlO ₁₀ (OH) ₂	14.14	Modelled
Chamosite	(Fe,Al,Mg,Mn) ₆ (Si,Al) ₄ O ₁₀ (OH) ₈	10.26	Not modelled
Calcite	CaCO ₃	3.80	Modelled
Vermiculite	Mg(Mg,Fe) ₃ (Si,Al) ₄ O ₁₀ (OH) ₂ .4H ₂ O	1.58	Not modelled
Dolomite	(Ca,Mg)CO ₃	1.10	Not modelled
Epidote	Ca ₂ (Al,Fe) ₃ (SiO ₂ O ₇)(SiO ₄)(OH) ₂	0.26	Not modelled
Albite	NaAlSi ₃ O ₄	BDL	No
Chlinochlore	Mg ₅ Al(Si,Al) ₄ O ₁₀	BDL	No
Gypsum	CaSO ₄ .2H ₂ O	BDL	No
Talcum	Mg ₃ Si ₄ O ₁₀ (OH) ₂	BDL	No
Aluminate	Al ₂ O ₃	BDL	No

* BDL - Below detection limit

Table 2 Homogeneous sandy aquifer characteristics

Parameter	Unit	Value	Range	Reference
Longitudinal dispersivity	m	5.06	3.0 - 15.24	(Gelhar et al. 1992)
			1.0 - 10	(Engesgaard et al. 1996)
Horizontal transverse dispersivity	m	0.45	0.01 - 10	(Gelhar et al. 1992; Shieh et al. 2010)
Vertical transverse dispersivity	m	0.015	0.01 - 10	
Hydraulic conductivity	m/s	5.17e-4	1.84e-4 - 7.05e-4 3.44e-4 - 8.37e-4	(Akhter and Hasan 2016)

Table 3 Typical municipal wastewater characteristics (Rehman et al. 2008; Sial et al. 2006)

Parameter		Unit	Value
pH		-	7.52
Arsenic	As	mg/l	0.94
Bicarbonate	C		9.5
Calcium	Ca		5.2
Cadmium	Cd		0.07
Chloride	Cl		1.3
Cobalt	Co		0.0003
Chromium	Cr		0.04
Copper	Cu		1.2
Iron	Fe		2.46
Potassium	K		18
Magnesium	Mg		5.2
Manganese	Mn		0.25
Nitrate	N(5)		28
Sodium	Na		18
Nickel	Ni		0.32
Lead	Pb		0.002
Sulphate	S(6)		517
Zinc	Zn		0.21

Table 4 Background infilling solution characteristics (Rasool et al. 2016a; Rasool et al. 2016b)

Parameter		Unit	Value
pH		-	7.32
Arsenic	As	mg/l	0.10
Bicarbonate	C		646
Calcium	Ca		127
Cadmium	Cd		0.07
Chloride	Cl		88
Cobalt	Co		0.0003
Chromium	Cr		0.04
Copper	Cu		0.04
Iron	Fe		1.12
Potassium	K		4
Magnesium	Mg		46
Manganese	Mn		0.01
Nitrate	N(5)		28
Sodium	Na		368
Nickel	Ni		0.03
Lead	Pb		0.09
Sulphate	S(6)		517
Zinc	Zn		0.86

Table 5 Parameters for numerical transport modelling

Parameter	Unit	Value	Reference
Transport Model			
Column length	m	100	-
Solids amount	g/l	4e3	
Longitudinal dispersivity	m	5.06	
Simulation timescale	y	100,000	
Quartz Dissolution Kinetics			
Initial moles (m_0)		102.7	(Sracek 2013)
Surface area (A_0)		22.7	
Solution volume (V)		0.162	
Calcite Dissolution/Precipitation Kinetics			
Initial moles (m_0)	mol	7e-4	(Parkhurst and Appelo 2013)
Area to volume ratio (A/V)	cm ² /l	5.0	
Exponent for m/m_0	-	0.3	
Arsenic Sorption Kinetics			
Initial moles (m_0)	mol	1e-8	-
Tolerance (tol)	mol	1e-1	

Table 6 Heavy metals concentrations at the end of the simulation time and their comparison with drinking water standards

Heavy Metals	Concentration at the end of the Simulation Time	Drinking Water Standards		
		WHO*	USEPA**	PEQS***
	mg/l			
As	3.79	0.01	-	≤0.05
Cd	0.07	0.003	0.005	0.01
Fe	1.95	0.3	0.3	-
Mn	0.16	0.5	-	≤0.5
Pb	0.04	0.01	0	≤0.05
Co	0.0003	0.001	0.002	≤0.001
Cr	0.04	0.05	0.1	≤0.05
Cu	0.75	2	1.3	2
Ni	0.21	0.02	-	≤0.02
Zn	0.46	3	5	5

* WHO, 2011

** USEPA, 2009

*** PEPD, 2019

† Blue highlighted values are above the standards.

Table 7 Inorganic ions concentrations at the end of the simulation time and the comparison with drinking water standards

Inorganic Ions	Concentration at the end of the Simulation Time mg/l	Drinking Water Standards		
		WHO*	USEPA**	PEQS***
C	263.47	500	-	-
Ca	57.65	100	-	200
Mg	20.68	75	-	-
N(5)	121.35	50	10	50
S(6)	517.23	500	-	500
Cl	34.30	250	-	250
K	12.59	12	-	-
Na	153.11	200	-	-

* WHO, 2011

** USEPA, 2009

*** PEPD, 2019

† Blue highlighted values are above the standards.

Table 8 Pearson correlation matrix for heavy metals and inorganic ions through the simulation time period of 100,000 years

	As	Cd	Fe	Mn	Co	Cr	Cu	Ni	Pb	Zn	C	Ca	N(5)	S(6)	Cl	K	Mg	Na
As	1																	
Cd	0.5172	1																
Fe	-0.5160	-0.9999	1															
Mn	-0.5160	-0.9999	1	1														
Co	0.5176	0.9998	-0.9998	-0.9998	1													
Cr	0.5184	0.9998	-0.9999	-0.9999	0.9999	1												
Cu	-0.5160	-0.9999	1	1	-0.9998	-0.9999	1											
Ni	-0.5160	-0.9999	1	1	-0.9998	-0.9999	1	1										
Pb	0.5160	0.9999	-1	-1	0.9998	0.9999	-1	-1	1									
Zn	0.5160	0.9999	-1	-1	0.9998	0.9999	-1	-1	1	1								
C	0.5219	0.9998	-0.9998	-0.9998	0.9996	0.9998	-0.9998	-0.9998	0.9998	0.9998	1							
Ca	0.5464	0.9953	-0.9953	-0.9953	0.9946	0.9954	-0.9953	-0.9953	0.9953	0.9953	0.9968	1						
N(5)	-0.9977	-0.5737	0.5725	0.5725	-0.5731	-0.5748	0.5725	0.5725	-0.5725	-0.5725	-0.5781	-0.6012	1					
S(6)	0.5130	0.9996	-0.9998	-0.9998	0.9995	0.9996	-0.9998	-0.9998	0.9998	0.9998	0.9995	0.9945	-0.5697	1				
Cl	0.5160	0.9999	-1	-1	0.9998	0.9999	-1	-1	1	1	0.9998	0.9953	-0.5725	0.9998	1			
K	-0.5160	-0.9999	1	1	-0.9998	-0.9999	1	1	-1	-1	-0.9998	-0.9953	0.5725	-0.9998	-1	1		
Mg	0.5160	0.9999	-1	-1	0.9998	0.9999	-1	-1	1	1	0.9998	0.9953	-0.5725	0.9998	1	-1	1	
Na	0.5160	0.9999	-1	-1	0.9998	0.9999	-1	-1	1	1	0.9998	0.9953	-0.5725	0.9998	1	-1	1	1

* Orange highlighted correlation is significant at the 0.05 level (2-tailed).

** Red highlighted correlation is significant at the 0.01 level (2-tailed).